Journal of Molecular Graphics and Modelling 29 (2011) 685–692

Contents lists available at ScienceDirect

Journal of Molecular Graphics and Modelling

journal homepage: www.elsevier.com/locate/JMGM

Studying the catechol binding cavity in comparative models of human dopamine D_2 receptor

Amirhossein Sakhteman[a,b,*], Maija Lahtela-Kakkonen[a], Antti Poso[a]

[a] School of Pharmacy, Faculty of Health Sciences, University of Eastern Finland, Kuopio, Finland
[b] Department of Medicinal Chemistry, Faculty of Pharmacy, Shahid Sadoughi University of Medical Sciences, Yazd, Iran

ARTICLE INFO

Article history:
Received 13 July 2010
Received in revised form
16 November 2010
Accepted 22 November 2010
Available online 2 December 2010

Keywords:
G protein coupled receptor
Conformational changes
Agonist binding cavity
Comparative modeling
Ligand screening

ABSTRACT

Obtaining more structural information of human dopamine D_2 receptor may help in the design of better therapeutic agents against diseases such as Parkinsons. In this study attempts have been made to develop a functional model for the catechol binding site of the human dopamine D_2 receptor, with two primary models being postulated based on the presence of a disulfide bridge in the second extracellular loop. The models have been subjected to subsequent molecular dynamics simulation and receptor based virtual screening of catechol structures. During steady state of the simulations, representative models with the reduced disulfide bridge were more capable of discriminating between active and inactive catechol structures. It is postulated that similar conformational changes of the second extracellular loop observed in 5-HT4 and β-adrenergic receptors, might also take place in the human D_2 receptor during its interaction with agonist ligands.

1. Introduction

Human dopamine D_2 receptors together with muscarine, serotonin, canabinoid and some other membrane proteins are categorized in class I GPCR (G protein coupled receptor) [1]. GPCRs are one of the largest group of cell surface membrane proteins [1]. A common feature of these receptors is their architecture which consists of seven transmembrane bundles [2]. The central position of GPCRs in many physiological activities means that they represent a therapeutic target in a wide spectrum of diseases [3]. For this reason it is important to obtain more knowledge about 3D structure and functionality of GPCRs [4,5]. Since these types of proteins are embedded within the membrane, the purification of sufficient amounts for X-ray crystallography has been remained a challenging problem for these types of receptors [5]. In addition, the poor aqueous solubility of membrane proteins makes it difficult to obtain crystal structures of GPCRs [6]. NMR studies of GPCRs have also encountered different types of problems. These problems occurred due to the formation of large protein detergent complexes and effects of a slow rotational correlation on T_2 relaxation properties of the protein [5]. Therefore, at present there are few reports of experimental based GPCR structures published. These receptors include bovine rhodopsin, β_2-adrenergic receptor, β_1-adrenergic receptor and adenosine A_2 receptor [7].

It has been claimed that malfunctions of the dopaminergic nerves may be involved in many diseases such as Parkinsons and psychosis [8]. More knowledge about the role and functionality of this receptor would be very useful for designing improved therapeutic agents. Since no experimental 3D structure of the dopamine D_2 receptor has been published. Modeling techniques in conjunction with experimental studies such as site directed mutagenesis data may be a useful tool for obtaining more structural information about this protein [5,9]. Early homology models of human D_2 receptors were based on the 3D structures of rhodopsin and bacteriorhodopsin. In some other studies *de novo* methods were used to model the entire receptor based on the constraint estimated for the interaction between the receptor and the membrane [10].

The emergence of the high resolution crystal structures of β-adrenergic receptor in 2007 inspired many researchers to use them as their main templates for modeling the D_2 receptor [11,12]. Further approaches have been used to achieve a more accurate view of this receptor and other GPCRs. The presence of a disulfide bridge in the second extracellular loop between Cys_{107} and Cys_{182} was verified by site directed mutagenesis data. This discovery was followed by an attempt to investigate the interaction of antagonists with the human dopamine D_2 receptor [13]. Furthermore, the handedness of the corresponding disulfide bridge in 5HT4 and different conformational behaviors of second extracellular loop (ECL_2) during interactions with agonists, antagonists and inverse agonists were revealed by circular dichroism (CD) studies [14].

* Corresponding author at: Department of Medicinal Chemistry, Faculty of Pharmacy, Shahid Sadoughi University of Medical Sciences, Yazd, Iran.
Tel.: +98 351 8203865.
E-mail address: asakhteman@razi.tums.ac.ir (A. Sakhteman).

1093-3263/$ – see front matter © 2010 Elsevier Inc. All rights reserved.
doi:10.1016/j.jmgm.2010.11.012

Based on these findings it was speculated that there might be some conformational changes in the second extracellular loop and binding cavity of D_2 receptor. Our subsequent attempt was to obtain a predictive model for the binding crevice of catechol agonists and therefore the human dopamine D_2 receptor was modeled both in the presence and absence of a disulfide bridge in the second extracellular loop. This strategy made it possible to investigate the role of handedness in the disulfide bridge as well as its role on conformational changes occurring within the agonist binding cavity. Further simulation of both models has been taken to stabilize the receptors in the membrane. Finally, the ability of both models to discriminate between active and inactive structures was evaluated by docking studies.

2. Methodology

All calculations were performed with 8 processors on a Rocks Linux cluster (node of 2 × 1.86 GHz Intel Quad-Core Xeon) equipped with a sun grid engine (SGE) queuing system.

2.1. Homology modeling

The sequence of the human short isoform dopamine subtype 2 receptor (Access Code P14456) was downloaded from www.expasy.org in FASTA format [15]. The BLAST search using BLOSUM62 scoring matrix, implemented in Discovery studio, was performed once on the whole receptor sequence and another time on the transmembrane and loop regions [2]. Three template structures (PDB code: 1lNL, 2RH1 and 1TDJ) were selected based on their homologue regions with D_2 receptor. Some manual modifications were undertaken by inserting or deleting the dashes in the alignment file. By these modifications, the identity of the final alignment increased to 42% (Fig. 1). The resulting multiple alignment file was used to make primary models of the receptors using Modeller 9v3 [16]. With regard to the probable formation of a disulfide bridge between the two residues Cys_{107} and Cys_{182}, two comparative models were proposed for D_2 receptor in this study [16]. The models were different in the way that the disulfide bridge was present in one model but ignored in the other (Fig. 2). In both cases, the best models were ranked based on Discrete Optimized Protein Energy (DOPE) score of the Modeller software [16]. The loop regions of the highest scored model with less homology in respect to templates were refined with the loop refinement script of Modeller

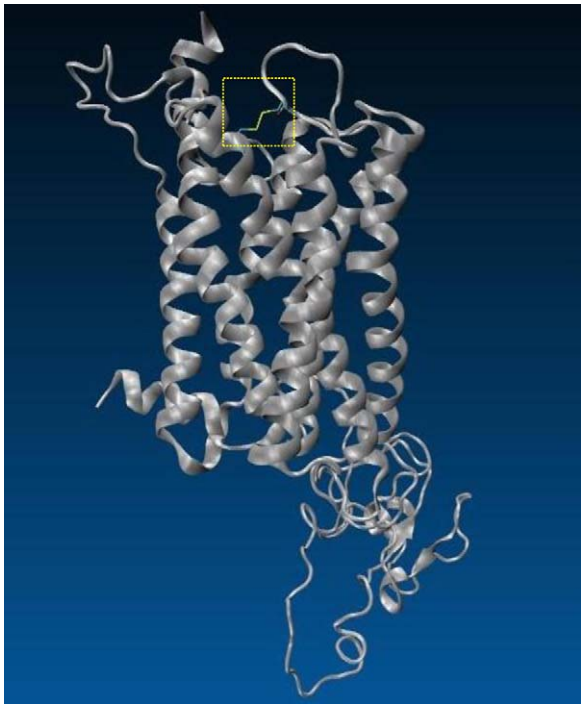

Fig. 2. Model of human D_2 receptor with retained disulfide bridge between Cys_{107} and Cys_{182}.

and the stereochemical quality of the models was evaluated using Procheck [17].

2.2. Molecular dynamics simulation

The final models have been subjected to molecular dynamics simulations using Desmond [18,19]. The protein wizard preparation was used to correct for structural defects, add hydrogens and assign tautomerization and ionization states. A DPPC bilayer membrane model was set up using TIP3P as a solvent and a physiological salt concentration of 0.15 M NaCl was introduced in to the system. In order to stabilize the modeled proteins within the membrane, two short (1.2 ns) simulations with 50 kcal/mol/Å^2 restraints on the protein residues were run for both models. The recording interval

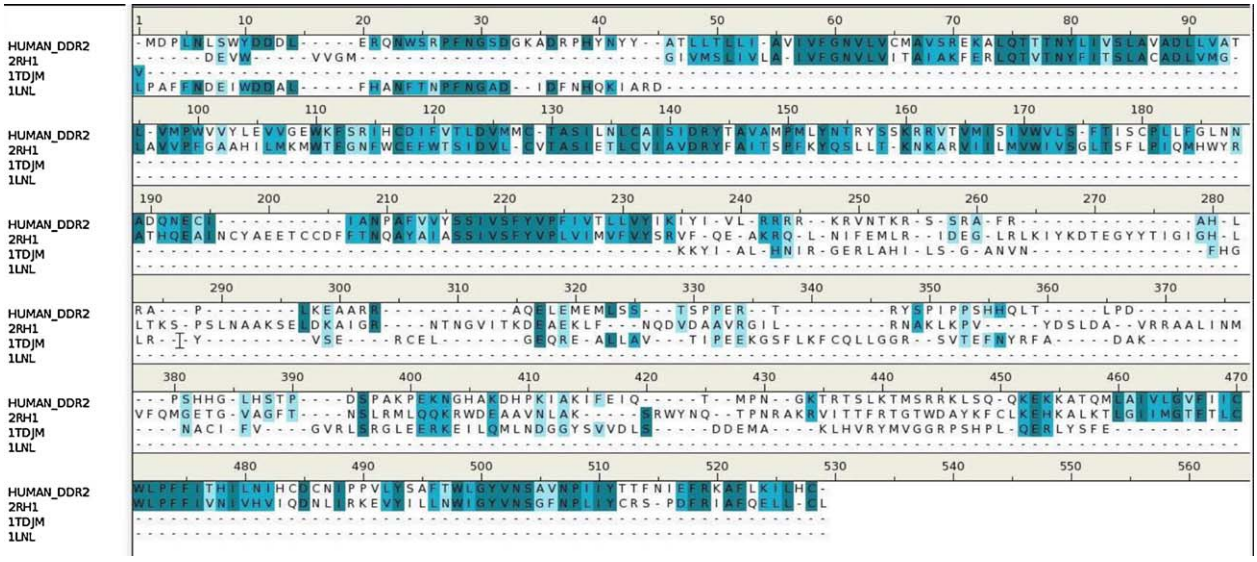

Fig. 1. Final multiple alignments used for comparative modeling of human D_2 receptor.

of simulation was set to 1.2 ps and the method used to constrain bonds to hydrogen atoms was SHAKE algorithm with a tolerance value of 1E−5. Each run of the simulation was preceded by a minimization step with maximum runs of 1000 and MD step of 100. The convergence threshold for minimization was set to 1 kcal/mol/Å. The minimization method was a hybrid of the steepest decent and limited-memory Broyden–Fletcher–Goldfarb–Shanno (LBFGS) algorithms. The procedure of minimization and simulation were repeated keeping the restraint on the proteins' backbone. The main runs of simulations were conducted after excluding all the restraints from the systems. All simulation runs were performed through NPT ensemble and Berendsen algorithm was used as both thermostat and barostat. The force field OPLS2005 was used during all experiments. In order to extract the representative frames for further studies, the trajectories were clustered by the trajectory cluster.py script (Schrodinger). For this purpose, a hierarchical cluster linkage method based on the average RMSD of the whole protein was calculated. The parameters including the number of clusters and the number of frequencies were set to 2, 2, respectively. Further analysis of the simulations frames in terms of measuring Ca–Ca distances was done by tcl scripting as implemented in VMD [20].

2.3. Virtual screening

2.3.1. Database preparation

A set of structures for which there was experimental data of dopaminergic activity was downloaded from EMBL database in SMILES format [21,22]. Iterative runs of Open Babel through a shell script provided a primary 3D generation of the ligands in SDF format. Chemfinder ultra within the Chemoffice package was used to extract ligands with a catechol substructure [23]. Subsequently, calculation of ionization states followed by minimization using OPLS2005 force field was performed with Ligprep and Epik was used as an ionizer [24]. A set of 39 active ligands and 39 inactive compounds was present in the final database. The criteria used for assigning the compounds as either active or inactive were comparisons of their activity with their corresponding positive and negative controls. Based on these criteria, a cutoff value of 600 nm was used for classification of compounds to active and inactive subgroups. The experimental activity vector of compounds was constructed as a combination of string values, "A" representing active and "I" representing inactive compounds.

2.3.2. Docking

The two programs, GOLD with four scoring functions (Goldscore, ASP, PLP, and Chemscore) and GLIDE with the scoring functions Glidescore and Glideemodel (in both SP and XP modes) were used to dock the 39 active and inactive structures [25–27]. Based on the site directed mutagenesis data, Ser_{193} was considered as the docking center in all of the screening studies. It should be noted that the number of genetic algorithm runs in GOLD was set to 100 while all other parameters have been remained default in both softwares. The default parameters could be found in the supplemental material.

2.3.3. Analysis

The best scoring pose of each ligand was selected for further analysis. The efficiency of screening was analyzed by using the receiver operating curve (ROC) [28]. The significance of each ROC_{AUC} value was checked by a chance confirmation test through random scrambling of activity vector for 100 times and recalculating the ROC_{AUC} value for each random vector [28]. If the original ROC_{AUC} value was higher than the maximum random ROC_{AUC} value the test was considered as significant. For the best obtained ROC curve a further enrichment factor was also calculated. The calculation of the best scores, ROC values, chance confirmation test, and enrichment factors were done by means of an application implemented in visual.NET. Visualization of the ligand protein complex has been performed using Hermes viewer of GOLD software and Maestro interface of Schrodinger package [29].

3. Results and discussion

The used alignment of template and model sequences is shown in Fig. 1. The main template used for modeling transmembrane regions and the loop sections was the β-adrenergic receptor (2RH1). The identity of 2RH1 for TM regions was 46%. For the first extracellular loop (residues 1–38), the loop region of hemocyanin (1LNL) was used as the template (identity 50%). The crystal structure of threonine deaminase (1TDJ) with the identity of 14/25 was used as the template for the third intracellular loop (Fig. 1).

Two comparative models were built: one without a disulfide bridge and the other with a retained disulfide bridge. Assessment of the stereochemical quality of both comparative models of human dopamine D_2 receptor in terms of the Ramachandran plot revealed that all residues in the TM region and approximately 90% of the total residues were in the most favored regions. Subsequently, the models were stabilized in the membrane and further studies of molecular dynamics simulations were performed. The plots of RMSD versus time for both systems are depicted in Fig. 3. It can be seen that the final simulation time for reaching a plateau in RMSD curve of the system with disulfide-bridge was 5 ns while for the system with reduced disulfide bridge, the simulation required to run for 20 ns in order to reduce fluctuations in RMSD curve. The reason for different stabilization times in the two systems can be attributed to the presence of imposed restraints in the system with the disulfide-bridge which binds ECL_2 to TM_5. After the simulation runs, the trajectories were clustered as 5 subgroups and the representative frame in each subgroup was selected based on the RMSD values. The representative frames were subjected to another minimization step with the described parameters and the two frames with fewer clashes in the Ramachandran plot were selected (Fig. 4). The selected frames were used in the virtual screening studies using different types of knowledge based and empirical scoring functions to evaluate the ligand-receptor complex. There are two metrics mostly used to evaluate the predictive ability of the models in virtual screening, the enrichment factor and the area under the curve (AUC) values of the receiver operating curve [28].

The higher AUC values of ROCs reflect better predictive abilities in the models. Enrichment factor (EF) is largely dependent on the number of active compounds in a database, and cannot be generalized to global scales [28]. Therefore EF was used merely for verification of the final model. AUCs of ROC for all representative frames and their corresponding scoring functions are listed in Table 1. It can be observed from Table 1 that all significant ROC values were related to the frames with the reduced disulfide bridge. It can be noted that the highest ROC values in the frames with reduced disulfide bridge are higher than their counterparts in models with retained disulfide bridge. The highest ROC value in this study was attributed to the knowledge based scoring function (ASP) for frame 3130 with no disulfide bridge. This result implies that the binding cavity of this model is better able to discriminate between active and inactive structures. Although correlations cannot be interpreted as causality, this model is probably a more realistic conformational state of the binding site which interacts with the agonists. Plot of EF versus score based ranked database is also depicted in Fig. 5. The enrichment curve shows that the early enrichment factor with the maximum possible value ($EF_{max} = 2$) was achieved with all calculated enrichment values being above the random region. The quality of docking was also visualized by

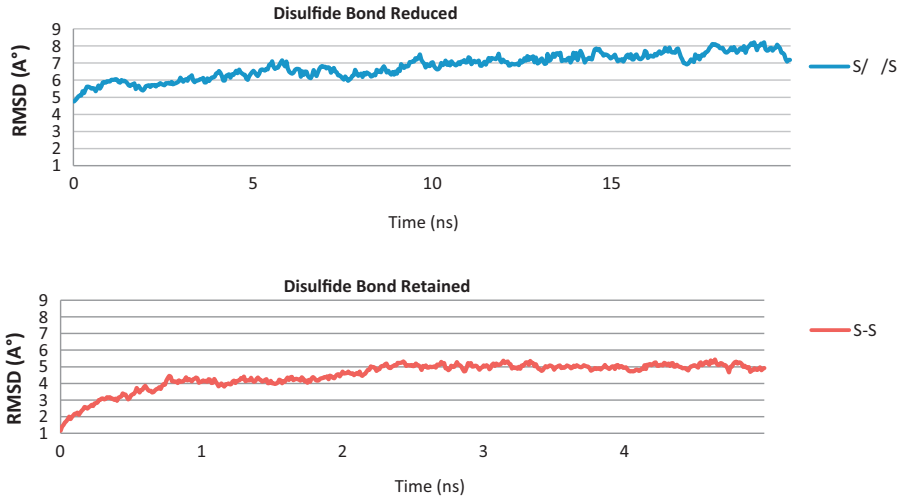

Fig. 3. RMSD plot of the two comparative models during molecular dynamics simulation.

Table 1
The area under the curve of ROC plots for representative frames of both models.

ROC_{AUC}		GOLD				GLIDE			
Cys_{107} Cys_{182}	Frame no.	Goldscore	ASP	PLP	Chemscore	SP		XP	
						Glidescore	Glideemodel	Glidescore	Glideemodel
Disulfide bridge reduced	2100	0.35	0.70*	0.70*	0.63	0.59	0.44	0.64	0.50
	3130	0.69*	0.80*	0.63	0.78*	0.50	0.45	0.70*	0.42
Disulfide bridge retained	380	0.29	0.50	0.50	0.54	0.43	0.45	0.40	0.59
	600	0.32	0.44	0.60	0.59	0.35	0.41	0.26	0.60

* Significant values in terms of chance correlation test.

the Hermes viewer in GOLD software. In order to perform a more reasonable validation test on the selected frames of the modeled proteins, a set of (10 ligands) with known EC50 values was used in the docking studies using Gold and Glide softwares. When finished with docking of the ligands, the correlation of the ligands in terms of the free energy scores with their corresponding log (1/EC50) values for each frame was calculated. In each case the correlation values are displayed in Table 2. It can be observed that the highest correlation was related to frame 3130 with the reduced disulfide bridge ($r = 0.92$) Therefore based on the docking studies, the binding cavity of frame 3130 is the most reliable model since it achieves a reasonable correlation coefficient. The important residues for the interaction of ligands and receptor have been identified based on the binding mode of active compounds (Fig. 6). The site finder module of MOE was used to obtain more convincing data about the geometry and feasibility of the binding site. Site finder is one of the geometrical methods for calculation of possible atom sites in a receptor from data about the 3D atomic

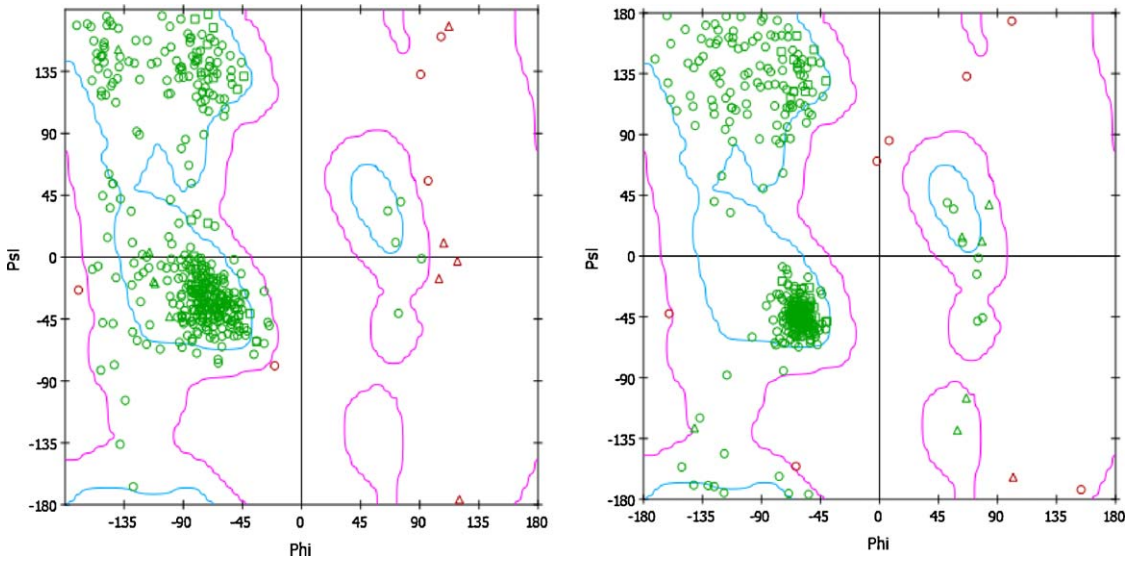

Fig. 4. Ramachandran plot of the model with retained disulfide bridge (left, frame 380), and the model with reduced disulfide bridge (right; frame 2400) during MD simulation.

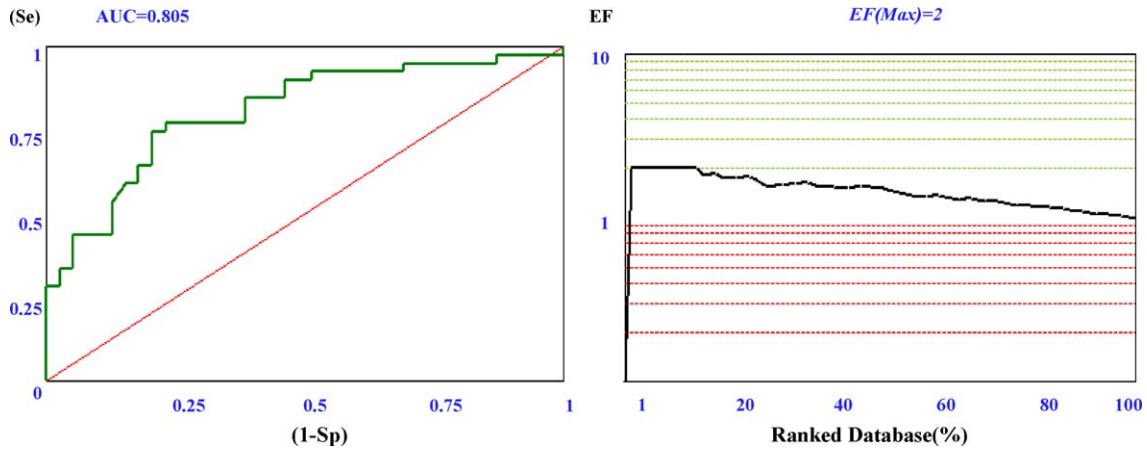

Fig. 5. ROC plot of virtual screening step with ASP scoring function for the model without disulfide bridge, frame 3130 (left), enrichment factor plot for the same model in logarithmic scale (right).

Table 2
Correlation (r) of the FEP values for the docked ligands with their corresponding −log(EC50) (-s//s- denotes the model lacking the disulfide bridge, -s-s- denotes the model keeping the disulfide bridge).

	-s//s-		-s-s-	
Selected frames	2100	3130	380	600
GOLD	0.83	0.92	0.67	0.77
GLIDE sp	0.61	0.6	0.63	0.59
GLIDE xp	0.62	0.57	0.54	0.57

coordinates of the protein. For this purpose a hydrophilic probe (1.4 Å) together with a hydrophobic one (1.8 Å) were used to scan the whole receptor. In this experiment, it was found that the site around the residues 115–114-193-185-379-183 was one of the most likely ones for undergoing interactions in this receptor (Fig. 7) [30].

As a way to investigate the effects of introducing a disulfide bridge on conformational changes of binding cavity, four residues taking part in the formation of binding cavity were selected for calculation of distances. The selection of the residues was made in such a way that the possible movement of TM3, TM6 and TM7 could be measured during the simulation. The residues selected were, Ser 193, Asn 114, Phe361 and Tyr 379 and they were located in TM5, TM3, TM6 and TM7, respectively. Ser193 is known to be an important residue in conjunction with Ser194 and Ser 197 in the binding of catechol structures according to several mutation studies [6]. When measuring the distances, Cα of the residue Ser193 was considered as the reference atom and the distances between

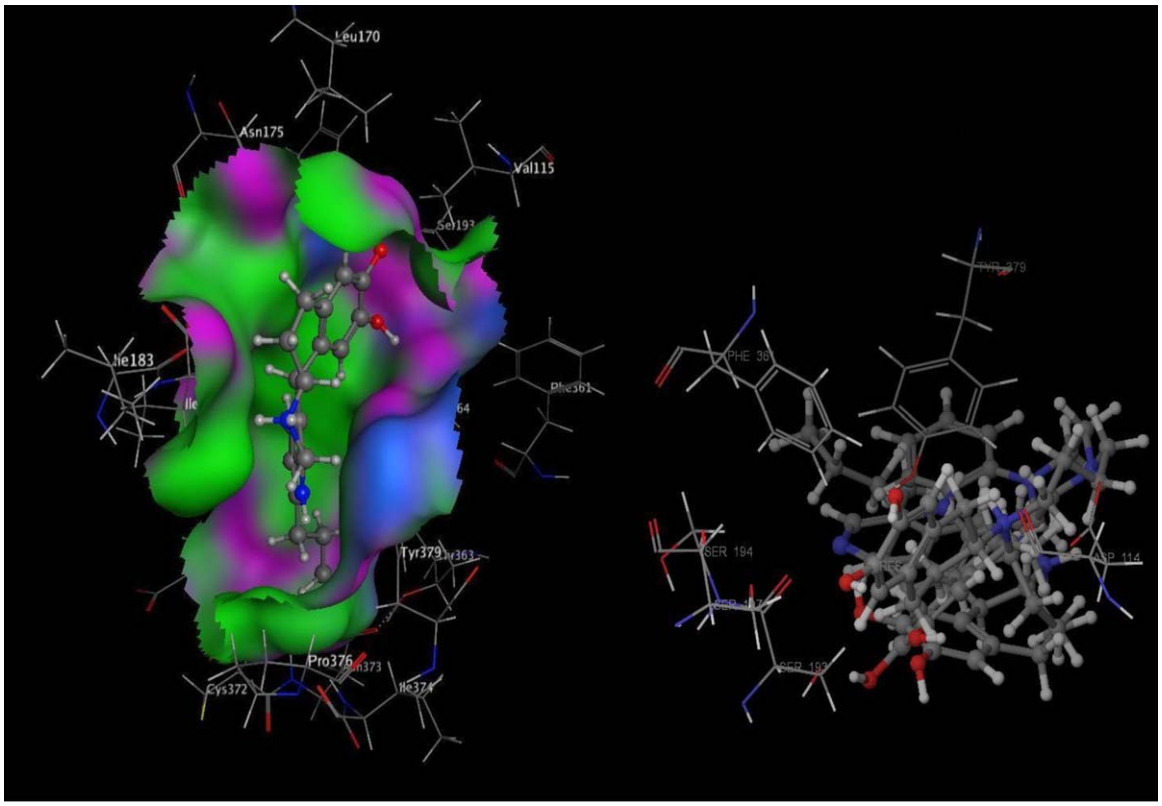

Fig. 6. Interaction of a catechol agonist in the binding cavity of model with reduced disulfide bridge (left, frame 3130). Binding mode of some active ligands in the same binding site (right). Docking was done with GOLD and scored with ASP function.

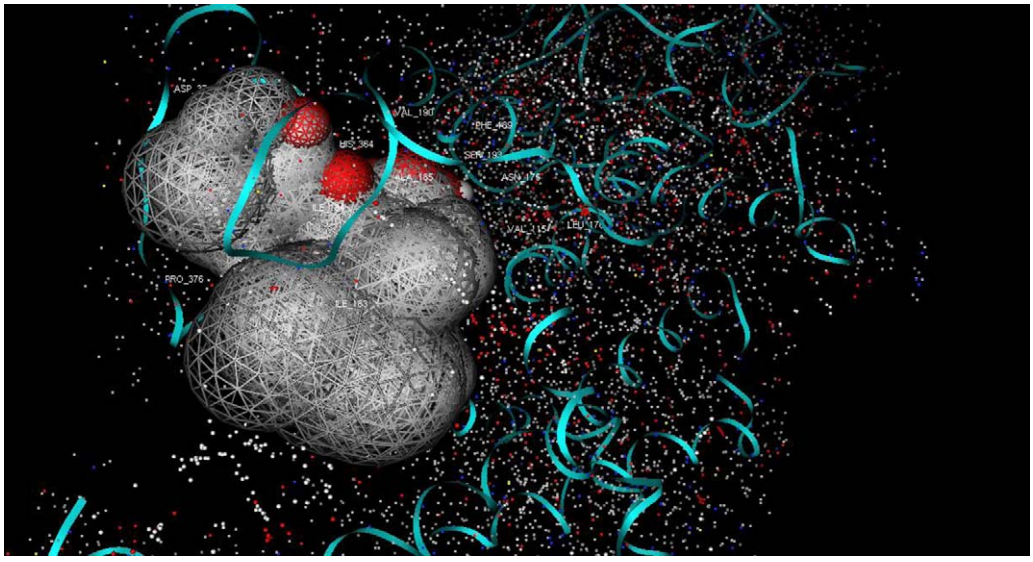

Fig. 7. A geometrical view of the binding site in human D_2 receptor for interaction of catechol structures. Grey areas denote the hydrophobic sites and the red areas denote the hydrophilic sites.

this and other selected residues (Cα) were calculated for all simulation trajectories. The plots of distances versus number of frame are depicted in Fig. 8. This reveals that for most of the simulation frames, the distances of the reference atom in TM_5 and selected residue in TM_6 for the model with reduced disulfide bridge is significantly less than the one with the presence of the disulfide bridge. In case of TM_5 and TM_3, there is less difference between the models, implying that a slight movement of transmembrane domains has occurred. On the other hand, measurement of the distances between the reference atom in TM5 and Cα of the residue 379 in TM7 detected that no significant difference between the two

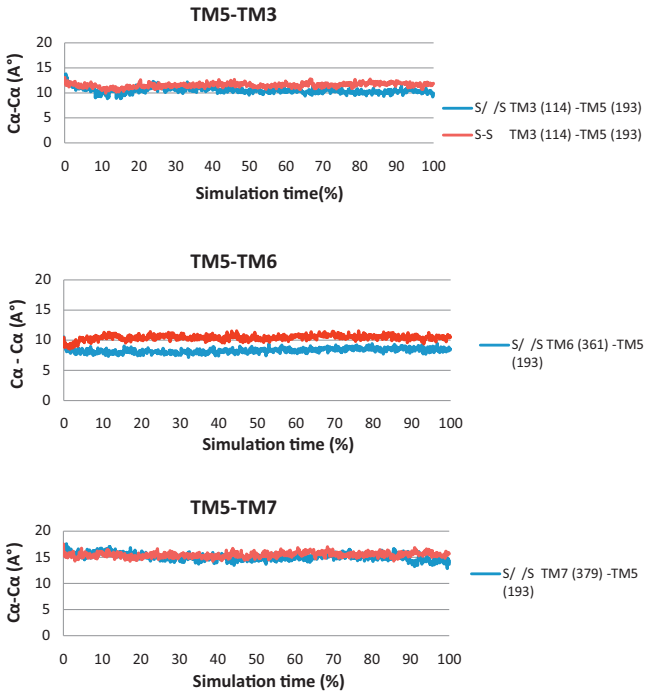

Fig. 8. Ca–Ca distances (Å) between reference atom (Ca of the residue Ser 193) and representative residues from different TM regions during simulation (model with retained disulfide bridge in red, model with reduced disulfide bridge in blue). (For interpretation of the references to color in this figure legend, the reader is referred to the web version of the article.)

comparative models had taken place. A superposition of the two representative models before and during simulation was used to visualize this effect (Fig. 9). Since a single alignment file has been used for both proteins, a near to zero RMSD can be observed before simulation (RMSD = 0.26). On the other hand, during the steady states of simulation, some changes appear to have taken place. These changes are mainly caused by movement of TM_6 towards TM_5. This observation is in accord with some experimental studies examining the interaction of agonists with the β-adrenergic receptor where movements of TM_5 and TM_6 during activation have been reported [3]. This result was also in a good agreement with CD studies of 5-HT4 receptor with respect to the handedness in disulfide bridge in different conformational states of binding for agonists and antagonists. Our virtual ligand screening data indicated that the pattern of interaction for ligands in the binding site was in good agreement with other reports of docking and mutation studies which have also emphasized the role of residues such as Ser193, Ser 194, Ser 197 and Asn 114 in the formation of the agonist binding cavity (Fig. 6) [6]. In order to obtain more information on flexibility and rigidity of the receptor around the binding site, trajectory files of the model with reduced disulfide bridge have been subjected to the trajectory analysis toolbox with the VMD software. The result for this study is depicted in Fig. 10. It can be observed that the RMSD variation of the residues around the binding site during the simulation is less than 2 Å.

Table 3
RMSD analysis of MD trajectories for both models; (-s//s- denotes the model lacking the disulfide bridge, -s-s- denotes the model keeping the disulfide bridge).

Segments of the human D_2 receptor	RMSD(-s//s-)	RMSD(-s-s-)
L1: 1–37	3.18 ± 0.744	3.745 ± 0.436
TM1: 38–60	0.743 ± 0.097	1.830 ± 0.236
L2: 61–71	0.687 ± 0.21	1.323 ± 0.14
TM2: 72–97	1.16 ± 0.140	1.528 ± 0.204
L3: 98–108	0.944 ± 0.3	1.692 ± 0.192
TM3: 109–130	1.527 ± 0.147	1.289 ± 0.124
L4: 131–151	1.530 ± 0.227	2.076 ± 0.221
TM4: 152–174	1.382 ± 0.145	1.484 ± 0.116
L5: 175–186	1.336 ± 0.304	2.949 ± 0.368
TM5: 187–210	1.084 ± 0.137	1.633 ± 0.159
L6: 211–344	5.921 ± 0.787	5.604 ± 0.807
TM6: 345–368	1.278 ± 0.262	1.630 ± 0.182
L7: 369–376	0.906 ± 0.164	1.509 ± 0.222
TM7: 377–400	1.269 ± 0.212	2.124 ± 0.158

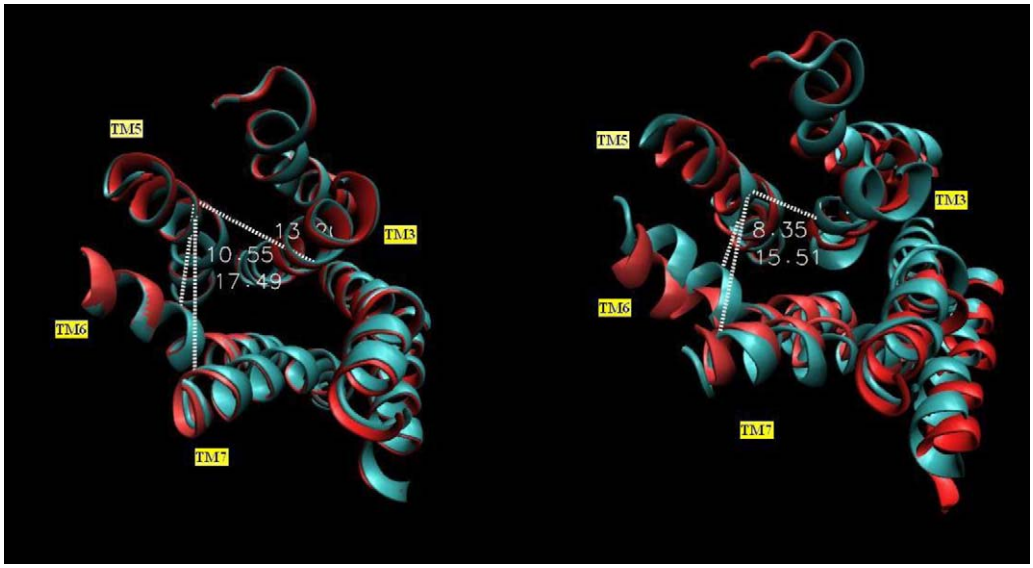

Fig. 9. Conformational change of agonist binding cavity: selected distances before simulation (left), during simulation (right). Model with reduced disulfide bridge (frame 3130) is depicted in red, model with retained disulfide bridge (frame 600) is depicted in cyan. The atoms used for distance calculations include Ca of Ser193 (TM5), Ca of Asn114 (TM3), Ca of Phe361 (TM6) and Ca of Tyr 379 (TM7). (For interpretation of the references to color in this figure legend, the reader is referred to the web version of the article.)

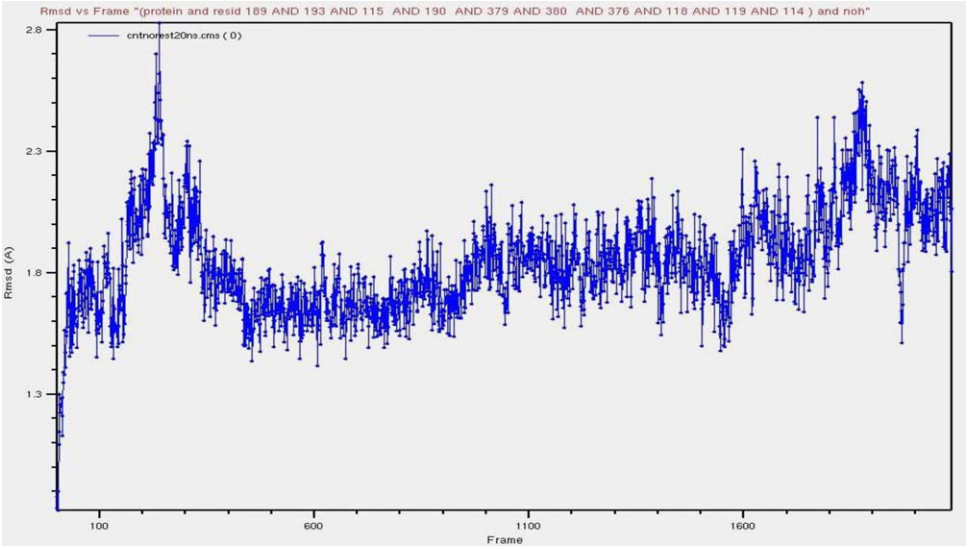

Fig. 10. RMSD variation of the residues constructing the binding site (189, 193, 115, 190, 379, 380, 376, 116, 119, 114).

The RMSD variation for each segment of the models was calculated separately and is displayed in Table 3. The maximum variation in RMSD of the segments for both models could be related to the 6th loop (residues 211–344) and the minimum variation was found in the 2nd loop (residues 61–71).

4. Conclusions

Two types of comparative models have been proposed for the human dopamine D_2 receptor. The models differ from each other in terms of the presence of a disulfide bridge between the second extracellular loop and TM_5. This was a convenient strategy to introduce conformational freedom in the disulfide site which is a requirement for the handedness of the disulfide bridge. The two models have been subjected to molecular dynamics simulations in a bilayer lipid membrane. Subsequently, the representative frames of each model have been subjected to virtual screening using a set of active and inactive compounds with catechol substructures. It was observed that a more predictive model for the catechol binding site was found in the system with the reduced disulfide bridge. This result was mainly due to movement of TM_6 with respect to TM_5 in the model with the reduced disulfide bridge. These findings point to the occurrence of conformational changes in the second extracellular loop of the receptor through the handedness of disulfide bridge. Therefore, it can be postulated that conformational change in the binding site might be due to the handedness of disulfide bridge. Similar results have been found in the cases of 5-HT_4 and β-adrenergic receptors [3].

Acknowledgment

The authors thank the Center for Scientific Calculations (CSC) in Finland for providing the software facilities for this work.

References

[1] J. Wess, S.J. Han, S.K. Kim, K.A. Jacobson, J.H. Li, Conformational changes involved in G-protein-coupled-receptor activation, Trends Pharmacol. Sci. 29 (2008) 616–625.

[2] N. Floquet, C. M'Kadmi, D. Perahia, D. Gagne, G. Berge, J. Marie, J.L. Baneres, J.C. Galleyrand, J.A. Fehrentz, J. Martinez, Activation of the ghrelin receptor is described by a privileged collective motion: a model for constitutive and agonist-induced activation of a sub-class A G-protein coupled receptor (GPCR), J. Mol. Biol. 395 (2010) 769–784.

[3] M.P. Bokoch, Y. Zou, S.G. Rasmussen, C.W. Liu, R. Nygaard, D.M. Rosenbaum, J.J. Fung, H.J. Choi, F.S. Thian, T.S. Kobilka, J.D. Puglisi, W.I. Weis, L. Pardo, R.S. Prosser, L. Mueller, B.K. Kobilka, Ligand-specific regulation of the extracellular surface of a G-protein-coupled receptor, Nature 463 (2010) 108–112.

[4] D.R. Flower, Modelling G-protein-coupled receptors for drug design, Biochim. Biophys. Acta 1422 (1999) 207–234.

[5] P.L. Yeagle, A.D. Albert, G-protein coupled receptor structure, Biochim. Biophys. Acta 1768 (2007) 808–824.

[6] M.Y. Kalani, N. Vaidehi, S.E. Hall, R.J. Trabanino, P.L. Freddolino, M.A. Kalani, W.B. Floriano, V.W. Kam, W.A. Goddard III, The predicted 3D structure of the human D2 dopamine receptor and the binding site and binding affinities for agonists and antagonists, Proc. Natl. Acad. Sci. U.S.A. 101 (2004) 3815–3820.

[7] T. Klabunde, C. Giegerich, A. Evers, Sequence-derived three-dimensional pharmacophore models for G-protein-coupled receptors and their application in virtual screening, J. Med. Chem. 52 (2009) 2923–2932.

[8] R.B. Tinsley, C.R. Bye, C.L. Parish, A. Tziotis-Vais, S. George, J.G. Culvenor, Q.X. Li, C.L. Masters, D.I. Finkelstein, M.K. Horne, Dopamine D2 receptor knockout mice develop features of Parkinson disease, Ann. Neurol. 66 (2009) 472–484.

[9] K. Kristiansen, Molecular mechanisms of ligand binding, signaling, and regulation within the superfamily of G-protein-coupled receptors: molecular modeling and mutagenesis approaches to receptor structure and function, Pharmacol. Ther. 103 (2004) 21–80.

[10] S. Shacham, Y. Marantz, S. Bar-Haim, O. Kalid, D. Warshaviak, N. Avisar, B. Inbal, A. Heifetz, M. Fichman, M. Topf, Z. Naor, S. Noiman, O.M. Becker, PREDICT modeling and in-silico screening for G-protein coupled receptors, Proteins 57 (2004) 51–86.

[11] V. Cherezov, D.M. Rosenbaum, M.A. Hanson, S.G. Rasmussen, F.S. Thian, T.S. Kobilka, H.J. Choi, P. Kuhn, W.I. Weis, B.K. Kobilka, R.C. Stevens, High-resolution crystal structure of an engineered human beta2-adrenergic G protein-coupled receptor, Science 318 (2007) 1258–1265.

[12] S.G. Rasmussen, H.J. Choi, D.M. Rosenbaum, T.S. Kobilka, F.S. Thian, P.C. Edwards, M. Burghammer, V.R. Ratnala, R. Sanishvili, R.F. Fischetti, G.F. Schertler, W.I. Weis, B.K. Kobilka, Crystal structure of the human beta2 adrenergic G-protein-coupled receptor, Nature 450 (2007) 383–387.

[13] L. Shi, J.A. Javitch, The second extracellular loop of the dopamine D2 receptor lines the binding-site crevice, Proc. Natl. Acad. Sci. U.S.A. 101 (2004) 440–445.

[14] J.L. Baneres, D. Mesnier, A. Martin, L. Joubert, A. Dumuis, J. Bockaert, Molecular characterization of a purified 5-HT4 receptor: a structural basis for drug efficacy, J. Biol. Chem. 280 (2005) 20253–20260.

[15] E. Gasteiger, A. Gattiker, C. Hoogland, I. Ivanyi, R.D. Appel, A. Bairoch, ExPASy: the proteomics server for in-depth protein knowledge and analysis, Nucleic Acids Res. 31 (2003) 3784–3788.

[16] N. Eswar, B. Webb, M.A. Marti-Renom, M.S. Madhusudhan, M.Y. Shen, U. Pieper, A. Sali, p Unit 29.

[17] R.A. Laskowski, M.W. MacArthur, D.S. Moss, J.M. Hornton, PROCHECK: a program to check the stereochemical quality of protein structures, J. Appl. Crystallogr. 26 (1993) 283–291.

[18] Desmond Molecular Dynamics System, Version 2.2, D.E. Shaw Research, New York, NY, 2009.

[19] Maestro-Desmond Interoperability Tools, Version 2.2, Schrödinger, New York, NY, 2009.

[20] W. Humphrey, A. Dalke, K. Schulten, VMD—Visual Molecular Dynamics, J. Mol. Graph. 14 (1996) 33–38.

[21] A. Hersey, A. Gaulton, L. Bellis, Y. Light, S. McGlinchey, ChEMBL DATABASE, 2009.

[22] J. Overington, ChEMBL. An interview with John Overington, team leader, chemogenomics at the European Bioinformatics Institute Outstation of the European Molecular Biology Laboratory (EMBL-EBI), J. Comput. Aided Mol. Des. 23 (2009) 198.

[23] R.E. Buntrock, ChemOffice Ultra 7.0, J. Chem. Inf. Comput. Sci. 42 (2002) 1505–1506.

[24] LigPrep, Version 2.3, Schrödinger, LLC, New York, NY, 2009.

[25] G. Jones, P. Willet, R.C. Glen, Molecular recognition of receptor sites using a genetic algorithm with a description of desolvation, J. Mol. Biol. 245 (1995) 43–53.

[26] G. Jones, P. Willet, R.C. Glen, Development and validation of a genetic algorithm for flexible docking, J. Mol. Biol. 267 (1997) 727–748.

[27] Glide, Version 5.5, Schrödinger, LLC, New York, NY, 2009.

[28] N. Triballeau, F. Acher, I. Brabet, J.P. Pin, H.O. Bertrand, Virtual screening workflow development guided by the "receiver operating characteristic" curve approach. Application to high-throughput docking on metabotropic glutamate receptor subtype 4, J. Med. Chem. 48 (2005) 2534–2547.

[29] Maestro, Version 9.0, Schrödinger, LLC, New York, NY, 2009.

[30] MOE, 2008,10, Chemical Computing Group, 2008.